



Somatic loss of *PIK3R1* may sensitize breast cancer to inhibitors of the MAPK pathway

Sanja B. Turturro¹ · Matthew S. Najor¹ · Timothy Yung¹ · Liam Portt¹ · Christopher S. Malarkey² · Abde M. Abukhdeir¹ · Melody A. Cobleigh¹

Received: 31 May 2019 / Accepted: 10 June 2019 / Published online: 17 June 2019
© Springer Science+Business Media, LLC, part of Springer Nature 2019

Abstract

Purpose The PI3K pathway, which includes the PI3K catalytic subunits p110 α (PIK3CA) and the PI3K regulatory subunit p85 α (PIK3R1), is the most frequently altered pathway in cancer. We encountered a breast cancer patient whose tumor contained a somatic alteration in PIK3R1. Some commercial sequencing platforms suggest that somatic mutations in PIK3R1 may sensitize cancers to drugs that inhibit the mammalian target of rapamycin (mTOR). However, a review of the preclinical and clinical literature did not find evidence substantiating that hypothesis. The purpose of this study was to knock out PIK3R1 in order to determine the optimal therapeutic approach for breast cancers lacking p85 α .

Methods We created an isogenic cellular system by knocking out both alleles of the PIK3R1 gene in the non-tumorigenic human breast cell line MCF-10A. Knockout cells were compared with wild-type cells by measuring growth, cellular signaling, and response to drugs.

Results We observed hyperphosphorylation of MEK in these knockouts, which sensitized PIK3R1-null cells to a MEK inhibitor, trametinib. However, they were not sensitized to the mTOR inhibitor, everolimus.

Conclusions Our findings suggest that breast cancers with loss of p85 α may not respond to mTOR inhibition, but may be sensitive to MEK inhibition.

Keywords BREAST CANCER · Cellular signaling · MEK · PIK3R1 · Trametinib

Introduction

Breast cancer is the most common cancer in women worldwide, with an estimated 1.6 million new cases reported annually [1]. Considerable attention has focused on the PI3K

signaling cascade following the discovery that *PIK3CA* is mutated in 30–50% of breast cancers [2–4]. *PIK3R1* encodes the regulatory domain (p85 α) of the PI3K complex. Several studies have demonstrated that expression of *PIK3R1* is downregulated in human cancers [5, 6], which can lead to tumor formation [5]. *PIK3R1* is one of several genes found to be differentially expressed in invasive ductal carcinoma of the breast compared to normal tissue [7]. A study of renal cell carcinoma found that *PIK3R1* downregulation leads to propagation and migration of renal cancer cells [8]. A study by Cizkova et al. [6] found that p85 underexpression is an independent negative prognostic factor in breast cancer. Taken together, these studies suggest that *PIK3R1* is a tumor suppressor.

Interest in personalized medicine has led to the emergence of commercially available tests that molecularly profile tumors in the clinical setting. These tests evaluate the mutational status of the most frequently mutated genes across all cancers [9]. Treating physicians receive a report of altered genes, which could be biomarkers of response to

Electronic supplementary material The online version of this article (<https://doi.org/10.1007/s10549-019-05320-x>) contains supplementary material, which is available to authorized users.

Sanja B. Turturro and Matthew S. Najor have contributed equally to this work.

✉ Abde M. Abukhdeir
abde_abukhdeir@rush.edu

¹ Division of Hematology, Oncology, and Cell Therapy, Department of Internal Medicine, Rush University Medical Center, 1725 W. Harrison St., Chicago, IL 60612, USA

² School of Pharmacy, Rueckert-Hartman College for Health Professions, Regis University, 3333 Regis Boulevard, H-28, Denver, CO 80221-1099, USA

FDA-approved drugs in that cancer type [9]. The theoretical efficacy of such agents is usually not validated in clinical trials and sometimes not even preclinically. As an example, we received a report from a commercially available molecular profiling panel on the cancer of a 50-year-old woman with metastatic breast cancer. The report noted a genetic alteration in *PIK3R1* and recommended everolimus as a rational treatment. We wondered whether this suggestion could be validated preclinically.

Limited preclinical evidence suggests that naturally occurring neomorphic *PIK3R1* mutations activate the MAPK pathway, suggesting therapeutic response to MAPK pathway inhibitors [10]. However, many genetic alterations in *PIK3R1* will result in complete loss of *PIK3R1*, as reported by these authors. Therefore, we aimed to create a model of pure *PIK3R1* loss in breast cancer, which was not confounded by alterations in other genes, to determine the efficacy of various FDA-approved drugs, including everolimus in breast cancers carrying loss-of-function mutations in *PIK3R1*.

Materials and methods

Patient history

A 50-year-old premenopausal executive was diagnosed with bilateral breast cancer on 6/16/14. Biopsy of the right breast revealed infiltrating ductal cancer, grade 2, estrogen receptor (ER) 99%, progesterone receptor (PR) 40%, HER2-negative. Biopsy of the left breast revealed infiltrating lobular carcinoma, grade 2, ER 85%, PR 35%, HER2-negative. She had germline testing in 2014 (Myriad Genetics; Salt Lake City, Utah). Full-length sequencing and full gene rearrangement analysis of BRCA 1 & 2 revealed no pathogenic mutations.

She underwent bilateral mastectomies and bilateral sentinel node biopsies. The right breast was stage pT2N1a and the left was pT1N0(i+) using the AJCC 7th edition. She received adjuvant doxorubicin (60 mg/M² and cyclophosphamide 600 mg/M, every 2 weeks × 4 cycles followed by dose-dense paclitaxel 175 mg/M² every 2 weeks × 4 cycles, completing chemotherapy in December 2014. Adjuvant tamoxifen was started in Jan 2015. By September 2015, she developed fatigue and right upper quadrant abdominal pain. Staging work-up revealed extensive hepatic metastatic disease, pleural effusion, and abdominal lymphadenopathy.

On 12/8/2015, ultrasound-guided core needle biopsy of the liver revealed metastatic breast cancer, ER 95%, PR the 45%, and HER2-negative by fluorescence in situ hybridization. Serum CA 27.29 was 5,941. On 12/11/15, carboplatin AUC 5 every 3 weeks IV and gemcitabine 1000 mg/M² days 1 and 8 every 3 weeks IV were started. By 1/18/16, after 2 cycles of chemotherapy, she achieved a partial response by

RECIST criteria. She received another four cycles of chemotherapy, ending 3/31/2016. Chemotherapy was discontinued after maximal chemotherapy response was achieved. Maintenance endocrine therapy was then started. On 4/15/16, she underwent bilateral salpingo-oophorectomy and on 4/21/16 started palbociclib and fulvestrant. By 9-1-16, progressive disease was documented in liver and pleura.

On 9-9-16, she underwent video-assisted thoracoscopy, drainage of right pleural effusion (2500 mL), right pleural biopsies, and insertion of PleurX catheter. Pleural biopsy revealed metastatic tissue that was sent for the NCI-MATCH trial (NCT02465060). There was no match.

On October 10, 2016 carboplatin was resumed, but she developed dose-limiting thrombocytopenia that precluded further treatment with carboplatin after 12-15-16. By 12-29-16, a CT scan showed progressive disease in the liver.

Cell culture

All cells were obtained from American Type Culture Collection (Manassas, VA). The non-tumorigenic human breast epithelial cell line MCF-10A and its derivatives were grown in a humidified atmosphere, supplemented with 5.1% CO₂ at 37 °C in a 50/50 mixture of Dulbecco's Modified Eagle Medium (DMEM) and Ham's Medium (DMEM:F12) devoid of phenol-red (Life Technologies, Grand Island, NY) supplemented with 5% horse serum (Sigma, Saint Louis, MO), 1% penicillin and streptomycin (Life Technologies, Grand Island, NY), 20 ng/ml epidermal growth factor (EGF) (Sigma, Saint Louis, MO), 10 µg/ml insulin (Sigma, Saint Louis, MO), 0.5 µg/ml hydrocortisone (Sigma, Saint Louis, MO), and 0.1 µg/mL cholera toxin (Sigma, Saint Louis, MO) (hereafter referred to as "supplemented medium") as previously described [11]. Gene-targeted cells were grown in supplemented medium, plus the addition of 0.4 µg/ml of puromycin (Sigma-Aldrich, St. Louis, MO) for 14 days during clonal selection. HEK-293T cells were grown in DMEM (Life Technologies, Grand Island, NY) supplemented with 5% fetal bovine serum (FBS; Sigma, St. Louis, MO) and 1% penicillin and streptomycin (Life Technologies, Grand Island, NY). MCF-10A cells and its derivatives used in assays and immunoblotting were performed in "assay medium," whereby horse serum was replaced with 1% charcoal-dextran-treated fetal bovine serum (CD-FBS; Fisher Scientific, Pittsburg, PA). All cells were harvested using Tryple Express (Life Technologies, Grand Island, NY). The cancer cell lines BT474 and MDA-MB-468 were grown in either RPMI or DMEM supplemented with 10% FBS and 1% penicillin and streptomycin, respectively. Assays on cancer cells were performed in their respective culture medium. All experiments using cell lines were performed within 6 months of resuscitation from initial freezing and were authenticated using short tandem repeat (STR) analysis at

The DNA Services Center within the Research Resources Center at The University of Illinois at Chicago. The latest STR analysis performed for MCF-10A cells was on July 21, 2015, BT-474 cells was on March 13, 2014, and MDA-MB-468 cells was on March 5, 2015.

Knockout of *PIK3R1* with CRISPR/Cas9

CRISPR/Cas9 was utilized to introduce a premature stop into exon 9, which is in the iSH2 domain of *PIK3R1*. This is the most frequently mutated region of *PIK3R1* and the first common exon across all splice variants, ensuring that all known splice isoforms of *PIK3R1* have been targeted [12]. The guide RNA (gRNA) target sequence (5'-GCTAGA GATTCATTCCGGTAG-3') was designed by GeneCopoeia (Rockville, MD) and subcloned into the plasmid LentiCRISPRV2 by Genscript (Piscataway, NJ). This guide was a top hit when used the online gRNA design tool crispr.mit.edu, with an on-target score of 84% and an off-target score of 83%. LentiCRISPRV2 (52961, Addgene, Cambridge, MA) devoid of a gRNA was used as an empty vector control.

Generation of lentiviral particles

The generation of lentiviral particles has been previously described [13]. HEK-293T cells were co-transfected with plasmids expressing psPAX2 (12260; Addgene, Cambridge, MA), VSVg plasmid (8454; Addgene, Cambridge, MA), LentiCRISPRV2 (Genscript, Piscataway, NJ) using Fugene HD transfection reagent (Promega, Madison, WI). The supernatant was collected and filtered using a 0.45 µm filter.

Infection and clonal selection

Purified viral particles were added to MCF-10A cells and supplemented with polybrene (Sigma-Aldrich, St. Louis, MO). After 24 h, virus-containing medium was removed; cells were washed with Hanks buffered saline solution (HBSS; ThermoFisher Scientific, Waltham, MA) and MCF-10A medium containing 0.4 µg/ml puromycin antibiotic selection was added to the cells. Clonal populations were derived from single cells by limited dilution cloning. Clones were analyzed by western blot to confirm the loss of p85α protein. Clones lacking p85α were PCR amplified using Platinum PCR SuperMix (Invitrogen; Grand Island, NY) and primers (5'-TCGAGATACAGCAGACGGGAC-3' and 5'-AATAAATGCTCTCACCCACC-3') that flanked the predicted Cas9-mediated cleavage site. The amplicon was subcloned into the TOPO®-TA vector (Invitrogen, Carlsbad, CA) and transformed into competent *E. Coli* cells according to the manufacturer's protocol. Individual bacterial colonies were grown in LB medium, mini-prepped, and Sanger sequenced to identify the sequence of each individual allele.

Growth proliferation assay

The small molecule inhibitor of mTOR, everolimus (RAD001), and MEK, PD0325901, and trametinib were purchased from Selleckchem (Houston, TX). Cell growth assays were performed as previously described [14]. Cellular clones were harvested, washed with HBSS (ThermoFisher Scientific, Waltham, MA) three times, and then seeded in EGF-free assay medium. After 24 h, cells were treated with 0.2 ng/mL EGF either alone or in combination with everolimus (RAD001), PD0325901, or trametinib. After 1 week, cellular density was assessed by either MTS (Promega; Madison, WI) or crystal violet (CV). The latter was performed by washing cells with DI water and then stained with 4.9 mM CV resuspended in 10% formalin. Plates were dried for at least 24 h before solubilization with 2 M acetic acid and then analyzed on a microplate reader at an absorbance of 580 nm. For each cellular clone, measurements were normalized to the respective initial cell counts. All assays and growth conditions were performed in triplicate.

Colony formation assay in semisolid medium and morphogenesis assay

The bottom layer of this two-layer system was prepared by pouring 2.0 ml of DMEM:F12 supplemented with 0.6% Ultrapur agarose in each well of a 6-well plate. Once solidified, 3.0×10^5 cells were suspended in 3.0 mL of supplemented DMEM:F12 containing 0.4% UltraPure Agarose (Invitrogen, Grand Island, NY) and poured over the bottom layer. After the top layer solidified, 2 ml of DMEM:F12 medium was added to each well and replaced weekly. After three weeks of incubation, wells were stained overnight with Nitro Blue Tetrazolium (Sigma, St. Louis, MO) [11]. The next day, cells were imaged using a VersaDoc imager (Bio-Rad, Hercules, CA). The morphogenesis assay was performed, as previously described. Images were acquired under a phase contrast microscope (Nikon, Tokyo, Japan) following 2 weeks of incubation.

Immunoblotting

Whole cell protein lysates were prepared, resolved, and immunoblotted as previously described [14]. Membranes were incubated with the primary antibodies p85 (SC-71892), phosphorylated AKT (4056 & 9271), total AKT (9272), phosphorylated ERK (9106), total ERK (9102), phosphorylated MEK 1/2 (9121), total MEK (9122), β-actin (12620), or GAPDH (5174) as instructed by the manufacturer's protocol. This was followed by incubation with either an anti-mouse (7076) or an anti-rabbit (7074) secondary antibody conjugated to horseradish peroxidase at a dilution of 1:3000. Protein bands were visualized using enhanced

chemiluminescent reagent (Perkin-Elmer, Waltham, MA). The anti-p85 antibody was purchased from Santa Cruz Biotechnology (Dallas, TX), while all other antibodies (phosphorylated AKT, total AKT, phosphorylated ERK, total ERK, phosphorylated MEK 1/2, total MEK, β -actin, GAPDH, and secondary antibodies) were purchased from Cell Signaling Technology (Beverly, MA). Image J (NIH) analysis software was used to quantify the density of each protein.

In-gel digestion

The target bands were cut into 1 mm³ slices and destained with 100 mM ammonium bicarbonate/acetonitrile (1:1, vol/vol), followed by reduction and alkylation with 20 mM dithiothreitol and 10 mM iodoacetamide, respectively. After overnight trypsin digestion at 37 °C, the tryptic peptides were extracted with 1:2 (vol/vol) 5% formic acid/acetonitrile and desalted by C18 tips prior to LC/MS analysis.

LC-MS/MS analysis and data process

Peptide samples were run on Thermo Fisher Orbitrap Velos Pro coupled with Agilent NanoLC system (Agilent, Santa Clara, CA) over a 30 min. gradient. The LC columns (15 cm \times 75 μ m ID, Zorbax 300SB-C18) were purchased from Agilent. Samples were analyzed with a 60 min. linear gradient (0–35% acetonitrile with 0.1% formic acid) and data were acquired in a data-dependent manner, in which MS/MS fragmentation is performed on the top 10 most intense peaks of every full MS scan.

RAW files were converted into .mgf files using MSConvert (from ProteoWizard). Database searches were carried out using Mascot server (from Matrix Science). A decoy human Uniprot database v.5/11/2017 (81,213 entries) containing the reverse sequences was appended to the database in order to reduce false-positive identification results. The parameters used for database searching were set up as follows: trypsin as the protease with a maximum of two missed cleavages allowed. Carbamidomethylation of cysteine was specified as a fixed modification and oxidation of methionine, deamination of asparagine and glutamine were included as variable modifications. The minimum peptide length was specified to be 5 amino acids. The mass error was set to 10 ppm for precursor ions and 20 m μ for fragment ions. Search results from six runs were imported into Scaffold (Ver 4.75, Proteome Software, Portland, OR) for further analysis.

To concentrate on the targeted protein, RAW files were also imported into Maxquant (v1.57) to validate the existence of truncated protein by applying a customized database containing only the truncated protein sequences with the same search parameters as Mascot search above.

Protein structure and prediction analysis

Secondary protein structure prediction of the iSH2 and nSH2 regions of native p85 α and p85 α E468_E469insRYLE were performed using the Phyre2 server. The amino acid sequences for native and E468_E469insRYLE p85 α are listed in Supplementary Fig. 1. Both proteins were modeled in the intensive mode. Protein structures were visualized and evaluated using pymol.

Statistical analyses

Statistical analysis was performed using an unpaired two-tailed Student's *t* test. A *p* value of less than 0.05 was considered significant.

Results

Creating an Isogenic model for PIK3R1 Loss

In order to isolate the effects of *PIK3R1* loss in breast cancer, we created an isogenic cell line model, whereby we knocked out (KO) both alleles of *PIK3R1* in the immortalized human breast epithelial cell line, MCF-10A. Immunoblotting confirmed loss of p85 α protein expression in both KO clones 1 and 2 (Fig. 1). We were able to determine the exact DNA sequence of each allele in the region flanking the cut site using Sanger sequencing (Supplemental Fig. 1). The sequence of clone 1 revealed the presence of two alleles, one carrying a 20 bp deletion and a 61 bp deletion in the other. Both deletions introduced nonsense codons. In clone 2, we were only able to detect one allelic variant, an indel, consisting of a 53 bp deletion and a 3 bp insertion. This variant resulted in the production of a premature stop codon shortly downstream of the deletion. Since this clone did not produce p85 protein, it was likely a homozygous indel.

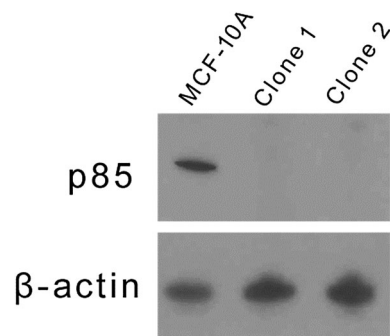


Fig. 1 Immunoblotting demonstrating loss of p85 protein expression in PIK3R1 knockout clones. MCF-10A (parental) and PIK3R1 knockout clones (1 and 2) were probed for p85 protein expression. β -actin was used as a loading control

Western blotting confirmed the absence of the full-length p85 α protein in both KO clones (Fig. 1). However, it was still possible for these targeted alleles to encode a truncated p85 α resulting from the nonsense mutation. Further analysis by western blot was unable to detect a truncated protein using an anti-p85 antibody with an epitope upstream of the Cas9 cut site (data not shown).

We reasoned that western blot analysis may not be sensitive enough to detect a truncated p85 α . Therefore, to further validate the absence of a truncated p85 α , we performed mass spectrometry on protein lysates of KO clones 1 and 2. None of the identified proteins matched any region of p85 α (including all splice variants; Supplemental Table 1). Taken together, the lack of protein expression observed by western blot analysis and the inability of mass spectrometry to generate a match to truncated p85 α , suggests that the nonsense codons in KO clones 1 and 2 were subjected to nonsense-mediated decay, leading to the complete loss of detectable p85 α .

Loss of PIK3R1 does not sensitize cells to mTOR inhibitors

Parental MCF-10A cells and their *PIK3R1* KO clones were subjected to increasing concentrations of the mTOR inhibitor everolimus (Supplemental Fig. 2). There was no statistically significant difference in response to everolimus observed between parental and KO clones, indicating that loss of p85 α did not sensitize cells to everolimus.

Loss of PIK3R1 leads to growth factor independence

The MCF-10A cell line requires EGF to proliferate. In the absence of EGF, these cells are growth arrested in G₁ [15]. In order to determine if loss of p85 α leads to growth independence from EGF, we performed cell growth assays in the presence and absence of EGF. Surprisingly, in the absence of EGF, clones 1 and 2 showed a statistically significant increase in proliferation, relative to the parental MCF-10A clone control (Fig. 2). When the cells were grown in the presence of 0.2 ng/ml EGF, both KO clones experienced a statistically significant increase in proliferation compared to the parental control cells, indicating increased growth stimulation by EGF (Fig. 2).

Colony and acinar formation

Parental MCF-10A cells are unable to form colonies in a semisolid medium [11]. However, loss of p85 α in both KO clones resulted in prominent colony formation (Fig. 3a–c). This demonstrates that loss of p85 α results in anchorage-independent growth, a phenotypic hallmark of malignant transformation. Parental MCF-10A cells form normal acini

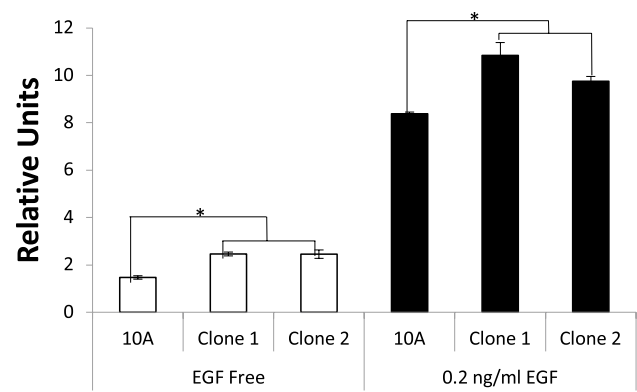


Fig. 2 Parental MCF-10A cells (10A) and two independently derived KO clones of MCF-10A lacking *PIK3R1* (Clones 1 and 2) expression were grown in the absence and presence of 0.2 ng/ml of EGF. Values are a mean \pm SD ($n=5$) * $p < 0.05$

in Matrigel (Fig. 3d). Loss of p85 α did not affect acinar formation, as both KO clones continued to form normal acini (Fig. 3e, f). Highly malignant cells often display abnormal acini formation. This finding suggests that loss of p85 α alone does not affect the organization of the cells.

MEK inhibitors retard growth of cells with PIK3R1 loss

We reasoned that loss of p85 α would result in activated PI3K because p85 α is the regulatory domain of the PI3K complex. We and others have previously reported that aberrant activation of PI3K results in increased signaling through the AKT, ERK, and MEK pathways [10, 16]. Thus, we used immunoblotting to examine the effect of p85 α loss on the levels of these proteins (Fig. 4). Parental MCF-10A cells require EGF for growth and withdrawal of EGF results in G₁ arrest. In parental MCF-10A cells, withdrawal of EGF results in nearly complete loss of phosphorylated AKT, MEK, and ERK proteins. Similar results were observed in both *PIK3R1* KO clones, as phosphorylated AKT and ERK were nearly undetectable (Fig. 4).

PIK3R1 KO clones grew faster than parental MCF-10A cells, suggesting that KO cells were more sensitive to EGF (Fig. 2). In order to determine which cellular signaling pathway was responsible for this, we stimulated the cells with EGF and measured phosphorylated AKT, MEK, and ERK proteins. Following EGF treatment, similar levels of activated AKT and ERK were observed. However, EGF treatment resulted in a marked increase in MEK activation in the knockout clones, compared to parental MCF-10A cells (Fig. 4).

Activated MEK is clinically “actionable,” therefore we treated *PIK3R1* null cells with either the small molecule inhibitor trametinib or PD0325901 to block aberrant MEK

Fig. 3 Colony formation assay depicting parental MCF-10A (a) and *PIK3R1* KO clones 1 and 2 (b and c). Parental MCF-10A cells form normal acini in matrigel (d). Loss of *PIK3R1* does not affect acini formation (e and f). Pictures are a single representation of ($n=3$)

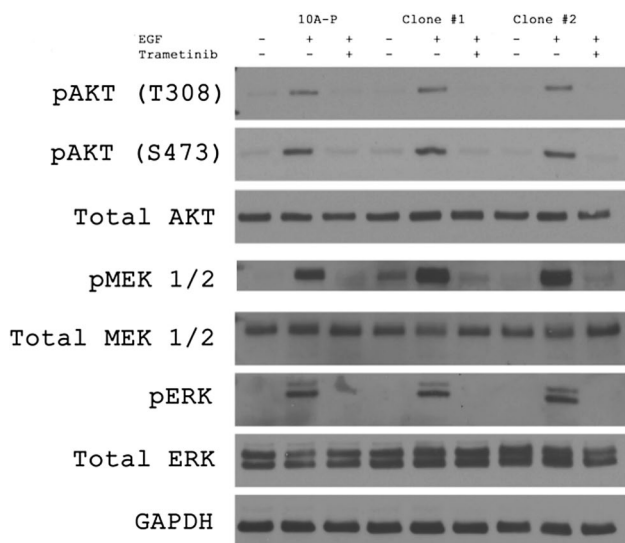
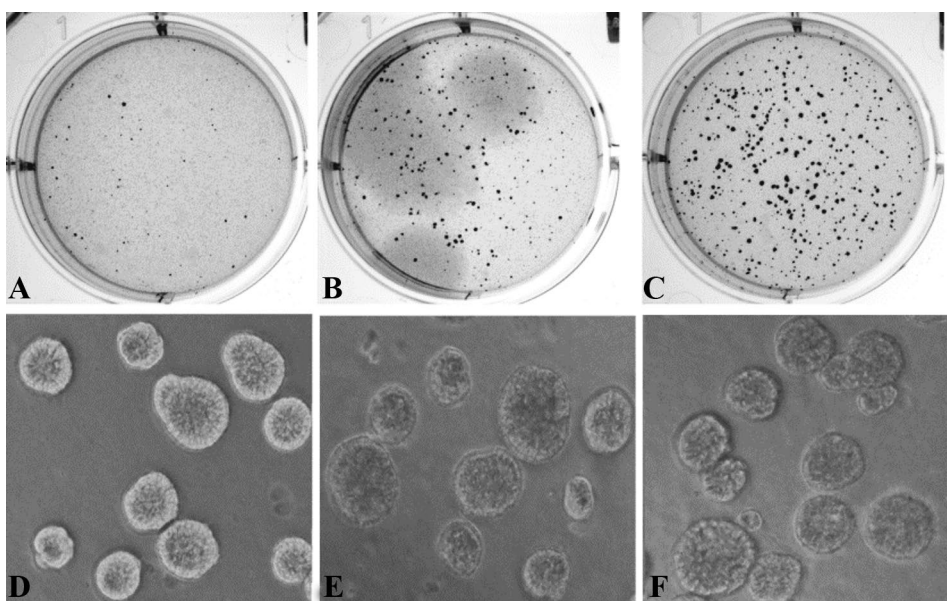


Fig. 4 MAPK signaling of MCF-10A (parental) and *PIK3R1* KO clones (1 and 2) in the presence and absence of 0.2 ng/ml EGF and 0.5 nM trametinib treatment. Blots are representative of $n=3$

activation. As seen from Fig. 4, treatment with trametinib blocked activation of EGF-stimulated MEK. Treatment of cells with trametinib resulted in dose-dependent inhibition of cellular growth. Loss of p85 α in the KO clones shifted the IC₅₀ of trametinib from 4.25 in parental clones to 0.275 and 0.7 nM for Clones 1 and 2, respectively (Fig. 5). Similar results were observed when cells were treated with PD0325901 (Supplemental Fig. 3). In order to determine if these findings were applicable to cancer cell lines, we tested the effects of trametinib in human breast cancer cell lines differing in p85 expression. As seen from Fig. 6,

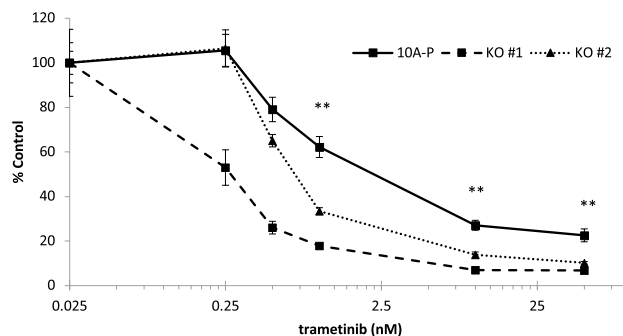


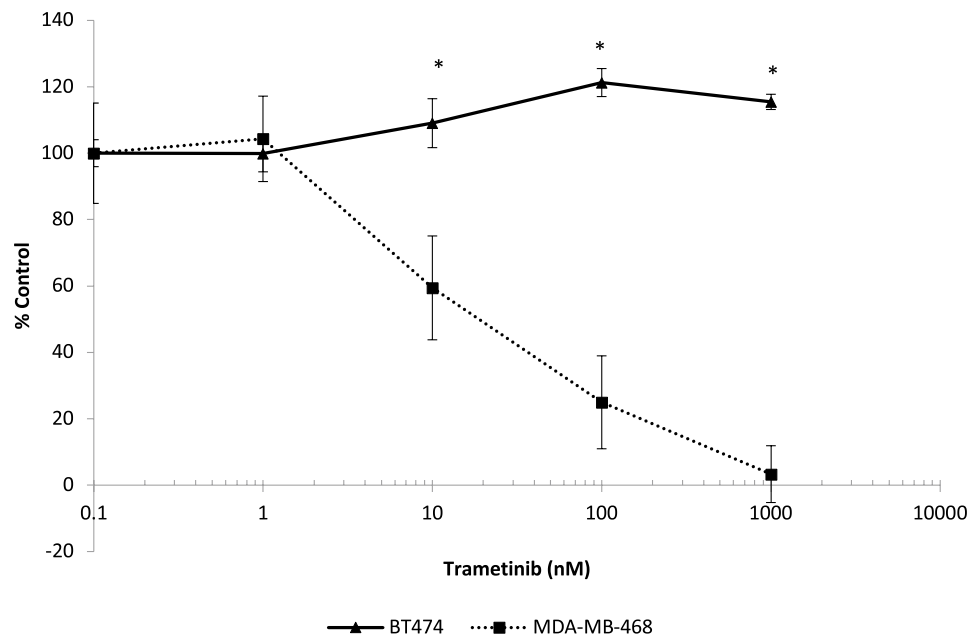
Fig. 5 Growth effects of the MEK inhibitor trametinib on parental MCF-10A and *PIK3R1* KO clones. Cells were treated with trametinib and 0.2 ng/mL EGF for 24 h. Values normalized to Day 0. Values are representation of mean \pm SD. ($n \geq 3$) $**p < 0.05$

MDA-MB-468 cells, which express low levels of p85 α are significantly more sensitive to trametinib than BT474 cells which express higher levels of p85. MDA-MB-468 cells achieved an IC₅₀ of 34.7 nM when treated with trametinib, while the BT474 cells were unaffected by trametinib concentrations as high as 1000 nM trametinib.

Somatic molecular profiling of patient's hepatic metastasis

Somatic molecular profiling of our patient's liver biopsy revealed the following alterations: *AKT3* amplification equivocal, *PIK3R1* E468_E469insRYLE, *PTEN* Loss of exons 6-9, *PALB2* E814*, and *G1121FS**3. Potential therapeutic agents suggested by the FoundationOne™ Assay (Foundation Medicine; Cambridge, MA) are summarized in Supplementary Table 2.

Fig. 6 Inhibitory effect of trametinib in cancer cells, MDA-MB-468 with downregulated PIK3R1 expression compared to BT474 cells. Values normalized to Day 0. Values are representation of mean \pm SD. ($n \geq 3$) * $p < 0.05$



In order to determine how the *PIK3R1* E468_E469insRYLE insertion might affect the interaction of p85 α with p110 α and lead to p110 α hyperfunction, we examined the known x-ray crystal structures of these protein complexes and modeled how the E468_E469insRYLE insertion might affect p85 α structure and function. The x-ray crystal structures of the nSH2 and iSH2 domains of p85 α bound to p110 α have been previously solved to a resolution of 2.96 Å. Both p110 α and p85 α have distinct structural regions that regulate the function of the respective proteins (Supplemental Fig. 4A). The insertion of four amino acids between residues E468 and E469 in *PIK3R1* of the patient's tumor (Supplemental Fig. 5) is consistent with the finding that most genetic alterations in *PIK3R1* associated with breast cancers are clustered between amino acids 456–469. The iSH2 and nSH2 domains are conserved across many proteins and are essential for protein–protein interactions. In order for p85 α to inhibit p110 α activation, the two long alpha helices of the iSH2 domain bind with the ABD, C2, helical, and kinase domains of p110 α and bring the nSH2 domain into contact with the C2 and helical domains of p110 α (Supplemental Fig. 4B). The iSH2 domain of p85 α cannot inhibit p110 α on its own and acts as a scaffold to bring the nSH2 domain into contact with the C2 and helical domains of p110 α to inhibit p110 α through an allosteric mechanism. It is therefore reasonable to assume that mutations in the iSH2 domain of p85 α that are essential for binding to p110 α would lead to decreased binding affinity for p110 α , and hence to increased p110 α activity. Indeed, it has been shown that mutations in the iSH2 domain of p85 α lead to p110 α hyperactivity in breast cancer. Since the *PIK3R1* E468_E469insRYLE insertion occurs at a region essential for binding of p85 α to

p110 α (Supplemental Fig. 4B), we modeled how the insertion might affect the protein structure using the Phyre2 protein homology modeling server (Supplemental Fig. 4C). The Phyre2 server makes predictions of protein secondary structure based on known structures in the protein data bank. The four amino acid insertions in the iSH2 domain of p85 α found in our patient could either increase the length of the alpha helix essential for binding to p110 α or induce a disorder kink in the alpha helix. The Phyre2 homology server predicts that the mutation introduces a disorder kink in the iSH2 alpha helix. In either case, a kink in the iSH2 alpha helix or an extension of the alpha helix would lead to disruption of the key interactions between the p85 α iSH2 domain and p110 α that theoretically allows the nSH2 domain to inhibit p110 α , causing aberrant kinase activity.

Discussion

PIK3CA is mutated in 30–50% of breast cancers, making it the most frequently mutated oncogene in breast cancer. Clinical studies have found that *PIK3CA* mutations are more prevalent in circulating tumor DNA of patients with metastatic breast cancer than in the primary tumors of the same patients and patients with mutant *PIK3CA* respond better to PI3K-inhibitors than do patients with wild-type PI3K ctDNA [17]. Among breast cancers that do not carry mutations in *PIK3CA*, dysregulation of the PI3K signaling axis can occur through mutations in *PIK3R1*. Mutations in *PIK3R1* and *PIK3CA* are mutually exclusive from each other [18]. Drug resistance to all therapies eventually occurs in patients with metastatic breast cancer and there is a need for additional

therapies to overcome resistance. Our results suggest that mutations in *PIK3R1* sensitize breast cells to inhibition of MEK. Taken together, targeting *PIK3R1* may offer a new approach in breast cancer therapy.

Effective targeted therapies require a priori knowledge of actionable biomarkers of response. *PIK3R1* is a tumor suppressor gene that is sporadically mutated, with the majority of the mutations occurring downstream of the iSH2 domain. Moreover, there are several splice variants of *PIK3R1*, which start transcription near the iSH2 domain. Therefore, we introduced a nonsense mutation near the iSH2 domain. This strategy eliminated all splice variants of *PIK3R1*. Both isolated clones resulted in complete ablation of p85 α protein expression, as determined by the combination of immunoblotting and mass spectrometry. Deletion of p85 α resulted in elevated levels of phosphorylated MEK and in EGF-independence. It is possible that aberrant MEK phosphorylation leads to EGF-independence, but this requires further investigation. This increase in MEK activation was found in our MCF-10A KO clones and in other breast cancer cell lines that lacked p85 α . Loss of p85 α sensitized these cells to the MEK inhibitor trametinib.

A study by Cheung et al. [10] found that mutations in *PIK3R1* sensitized endometrial cancer cells to the MEK inhibitor PD0325901. However, according to the authors, this drug was only effective when the *PIK3R1* mutation resulted in the production of a truncated protein, where the SH2 domain was still partially intact. The resulting phenotype of breast cancers carrying mutations in *PIK3R1* has never been studied. We reasoned that differences in the drug properties between PD0325901 and trametinib may account for the differences between our studies. Therefore, in addition to trametinib, we tested PD0325901 in the *PIK3R1* KO clones. Our results (Supplemental Fig. 3) are in contrast to the study by Cheung et al., where endometrial cells were only sensitive to MEK inhibition if the mutated transcript was able to express a truncated variant of p85 α , likely due to evading nonsense-mediated decay surveillance [10]. Consequently, they were able to observe the expression of the truncated protein with immunoblotting in the nuclear fraction of BaF3 cells that had been transfected with plasmids that encoded the truncated version of *PIK3R1* E160* or R348*. These discordant results in sensitivity observed in breast versus endometrial cells may be explained by different sites of mutation in the breast cancer cell lines we studied versus the endometrial cancer cell line they studied. We do not believe our results to be a clonal artifact, since MEK sensitivity was observed in two, independently derived clones of MCF-10A and the breast cancer cell line MDA-MB-468.

PD0325901 has shown activity in melanoma but proved too toxic for development [19–21]. Therefore, we explored the reversible MEK inhibitor trametinib. The advantages of trametinib include less toxicity and FDA approval for

use in patients with melanomas carrying BRAF mutations V600E and V600K. Complete loss of p85 α sensitized cells to trametinib; therefore, we wondered if the results reported by Cheung et al. may be specific to PD0325901. However, in our hands, complete knockout of p85 α also sensitized MDF-10A cells to PD0325901 (Supplemental Fig. 3).

The molecular profiling test on our patient's tumor also revealed genetic alterations in *PTEN* and *AKT*. The protein products of both genes are involved in the PI3K signaling pathway. It is possible that concurrent aberrations in multiple constituents of the PI3K signaling pathway render cells resistant to MEK inhibition (our patient was treated with trametinib for only 2 weeks before succumbing to her disease). This case underscores the complexity of human breast cancer, which often has multiple somatic alterations. Predicting treatment based on a single alteration may not be effective.

Our study confirms earlier reports that mutations in *PIK3R1* may lead to vulnerability through MEK inhibition. To the best of our knowledge, this is the first study to explore the use of MEK inhibitors in breast cancer cells carrying inactivating *PIK3R1* mutations. Moreover, we believe this to be the first study to explore the FDA-approved MEK inhibitor trametinib in a genetically predefined population of breast cancer cells. Our results provide evidence that genetically altered *PIK3R1* could be a biomarker for sensitivity to trametinib or to other MEK inhibitors in breast cancer and warrants exploration in animal models before beginning clinical trials.

Disclaimer The work herein was completed while AMA was a faculty member at Rush University. AMA is currently an employee with the U.S. Food and Drug Administration. The views and data in this publication do not reflect the opinions of The U.S. Food and Drug Administration.

Funding This study was funded by The Brian Piccolo Cancer Research Fund and Bears Care.

Compliance with ethical standards

Conflict of interest All authors declare no conflicts of interest.

Research involving human participants and/or animals This article does not contain any studies with human participants or animals performed by any of the authors.

Informed consent This article does not contain any studies with human participants performed by any of the authors.

References

1. Jemal A, Bray F, Center MM, Ferlay J, Ward E, Forman D (2011) Global cancer statistics. *CA Cancer J Clin* 61(2):69–90. <https://doi.org/10.3322/caac.20107>

2. Lauring J, Park BH, Wolff AC (2013) The phosphoinositide-3-kinase-Akt-mTOR pathway as a therapeutic target in breast cancer. *J Natl Compr Canc Netw* 11(6):670–678
3. Bachman KE, Argani P, Samuels Y, Silliman N, Ptak J, Szabo S, Konishi H, Karakas B, Blair BG, Lin C, Peters BA, Velculescu VE, Park BH (2004) The *PIK3CA* gene is mutated with high frequency in human breast cancers. *Cancer Biol Ther* 3(8):772–775
4. Samuels Y, Wang Z, Bardelli A, Silliman N, Ptak J, Szabo S, Yan H, Gazdar A, Powell SM, Riggins GJ, Willson JK, Markowitz S, Kinzler KW, Vogelstein B, Velculescu VE (2004) High frequency of mutations of the *PIK3CA* gene in human cancers. *Science* 304(5670):554
5. Taniguchi CM, Winnay J, Kondo T, Bronson RT, Guimaraes AR, Aleman JO, Luo J, Stephanopoulos G, Weissleder R, Cantley LC, Kahn CR (2010) The phosphoinositide 3-kinase regulatory subunit p85alpha can exert tumor suppressor properties through negative regulation of growth factor signaling. *Cancer Res* 70(13):5305–5315. <https://doi.org/10.1158/0008-5472.CAN-09-3399>
6. Cizkova M, Vacher S, Meseure D, Trassard M, Susini A, Mlucchova D, Callens C, Rouleau E, Spyrtos F, Lidereau R, Bieche I (2013) *PIK3R1* underexpression is an independent prognostic marker in breast cancer. *BMC Cancer* 13:545. <https://doi.org/10.1186/1471-2407-13-545>
7. Zhang BH, Liu J, Zhou QX, Zuo D, Wang Y (2013) Analysis of differentially expressed genes in ductal carcinoma with DNA microarray. *Eur Rev Med Pharmacol Sci* 17(6):758–766
8. Lin Y, Yang Z, Xu A, Dong P, Huang Y, Liu H, Li F, Wang H, Xu Q, Wang Y, Sun D, Zou Y, Zou X, Wang Y, Zhang D, Liu H, Wu X, Zhang M, Fu Y, Cai Z, Liu C, Wu S (2015) *PIK3R1* negatively regulates the epithelial-mesenchymal transition and stem-like phenotype of renal cancer cells through the AKT/GSK-3beta/CTNNB1 signaling pathway. *Sci Rep* 5:8997. <https://doi.org/10.1038/srep08997>
9. Chakravarty D, Gao J, Phillips S, Kundra R, Zhang H, Wang J, Rudolph JE, Yaeger R, Soumerai T, Nissan MH, Chang MT, Chandarlapaty S, Traina TA, Paik PK, Ho AL, Hantash FM, Grupe A, Baxi SS, Callahan MK, Snyder A, Chi P, Danila DC, Gounder M, Harding JJ, Hellmann MD, Iyer G, Janjigian YY, Kaley T, Levine DA, Lowery M, Omuro A, Postow MA, Rathkopf D, Shoushtari AN, Shukla N, Voss MH, Paraiso E, Zehir A, Berger MF, Taylor BS, Saltz LB, Riely GJ, Ladanyi M, Hyman DM, Baselga J, Sabbatini P, Solit DB, Schultz N (2017) OncoKB: a precision oncology knowledge base. *JCO Precis Oncol* 1:1–16. <https://doi.org/10.1200/PO.17.00011>
10. Cheung LW, Yu S, Zhang D, Li J, Ng PK, Panupinthu N, Mitra S, Ju Z, Yu Q, Liang H, Hawke DH, Lu Y, Broaddus RR, Mills GB (2014) Naturally occurring neomorphic *PIK3R1* mutations activate the MAPK pathway, dictating therapeutic response to MAPK pathway inhibitors. *Cancer Cell* 26(4):479–494. <https://doi.org/10.1016/j.ccell.2014.08.017>
11. Wang GM, Wong HY, Konishi H, Blair BG, Abukhdeir AM, Gustin JP, Rosen DM, Denmeade SR, Rasheed Z, Matsui W, Garay JP, Mohseni M, Higgins MJ, Cidado J, Jelovac D, Croessmann S, Cochran RL, Karnan S, Konishi Y, Ota A, Hosokawa Y, Argani P, Lauring J, Park BH (2013) Single copies of mutant KRAS and mutant PIK3CA cooperate in immortalized human epithelial cells to induce tumor formation. *Cancer Res* 73(11):3248–3261. <https://doi.org/10.1158/0008-5472.CAN-12-1578>
12. TCGA (2008) Comprehensive genomic characterization defines human glioblastoma genes and core pathways. *Nature* 455(7216):1061–1068. <https://doi.org/10.1038/nature07385>
13. Sanjana NE, Shalem O, Zhang F (2014) Improved vectors and genome-wide libraries for CRISPR screening. *Nat Methods* 11(8):783–784. <https://doi.org/10.1038/nmeth.3047>
14. Turturro SB, Najor MS, Ruby CE, Cobleigh MA, Abukhdeir AM (2016) Mutations in *PIK3CA* sensitize breast cancer cells to physiologic levels of aspirin. *Breast Cancer Res Treat* 156(1):33–43. <https://doi.org/10.1007/s10549-016-3729-8>
15. Ignatoski KM, Lapointe AJ, Radany EH, Ethier SP (1999) erbB-2 overexpression in human mammary epithelial cells confers growth factor independence. *Endocrinology* 140(8):3615–3622. <https://doi.org/10.1210/endo.140.8.6939>
16. Gustin JP, Karakas B, Weiss MB, Abukhdeir AM, Lauring J, Garay JP, Cosgrove D, Tamaki A, Konishi H, Konishi Y, Mohseni M, Wang G, Rosen DM, Denmeade SR, Higgins MJ, Vitolo MI, Bachman KE, Park BH (2009) Knockin of mutant *PIK3CA* activates multiple oncogenic pathways. *Proc Natl Acad Sci USA* 106(8):2835–2840
17. Baselga J, Im SA, Iwata H, Cortes J, De Laurentiis M, Jiang Z, Arteaga CL, Jonat W, Clemons M, Ito Y, Awada A, Chia S, Jagiello-Gruszfeld A, Pistilli B, Tseng LM, Hurvitz S, Masuda N, Takahashi M, Vuylsteke P, Hachemi S, Dharan B, Di Tomaso E, Urban P, Massacesi C, Campone M (2017) Buparlisib plus fulvestrant versus placebo plus fulvestrant in postmenopausal, hormone receptor-positive, HER2-negative, advanced breast cancer (BELLE-2): a randomised, double-blind, placebo-controlled, phase 3 trial. *Lancet Oncol* 18(7):904–916. [https://doi.org/10.1016/S1470-2045\(17\)30376-5](https://doi.org/10.1016/S1470-2045(17)30376-5)
18. Cancer Genome Atlas N (2012) Comprehensive molecular portraits of human breast tumours. *Nature* 490(7418):61–70. <https://doi.org/10.1038/nature11412>
19. LoRusso PM, Krishnamurthy SS, Rinehart JJ, Nabell LM, Malburg L, Chapman PB, DePrimo SE, Bentivegna S, Wilner KD, Tan W, Ricart AD (2010) Phase I pharmacokinetic and pharmacodynamic study of the oral MAPK/ERK kinase inhibitor PD-0325901 in patients with advanced cancers. *Clin Cancer Res* 16(6):1924–1937. <https://doi.org/10.1158/1078-0432.CCR-09-1883>
20. Haura EB, Ricart AD, Larson TG, Stella PJ, Bazhenova L, Miller VA, Cohen RB, Eisenberg PD, Selaru P, Wilner KD, Gadgil SM (2010) A phase II study of PD-0325901, an oral MEK inhibitor, in previously treated patients with advanced non-small cell lung cancer. *Clin Cancer Res* 16(8):2450–2457. <https://doi.org/10.1158/1078-0432.CCR-09-1920>
21. Boasberg PD, Redfern CH, Daniels GA, Bodkin D, Garrett CR, Ricart AD (2011) Pilot study of PD-0325901 in previously treated patients with advanced melanoma, breast cancer, and colon cancer. *Cancer Chemother Pharmacol* 68(2):547–552. <https://doi.org/10.1007/s00280-011-1620-1>

Publisher's Note Springer Nature remains neutral with regard to jurisdictional claims in published maps and institutional affiliations.